Axial behaviour of hollow core micropiles under monotonic loading

Ahmed Yehia Abd Elaziz, PhD Candidate,
M.Hesham Elnaggar, PhD, PEng, Professor, Research Director
Geotechnical Research Center, Department of Civil and Environmental Engineering, University of Western Ontario, London, Ontario, Canada,

ABSTRACT
Hollow bar construction, also termed self drilled, is becoming a popular option because it allows faster installation process and ground improvement at the same time. This paper presents a field study on the behaviour of single hollow core micropiles in stiff silty clay deposits. Four hollow core micropiles were installed using air flushing technique employing large drilling carbide bits. Five axial tests were conducted on the four micropiles; includes three compression and two tension monotonic axial tests. The results of the full-scale loading test performed on the micropiles are presented and analyzed in terms of load displacement curves. The results of the monotonic test show that the geotechnical bond strength values suggested by the FHWA implantation manual (2000) for the silty clay deposits may be underestimated when considering hollow core micropiles as Type B micropile grouting.

RÉSUMÉ
Hollow bar construction, parfois appelée "auto percés" - devient une option très populaire car elle permet un processus d'installation plus rapide et amélioration des sols en même temps. Cet article présente une étude de terrain sur le comportement des micropieux seule âme creuse dans raides dépôts limono-argileux. Quatre micropieux noyau creux ont été installés à l'air de rinçage technique qui utilise de grandes lames au carbure de forage. Cinq essais ont été réalisés axiale sur les quatre micropieux: comprend trois de compression et deux tests de tension monotone axiale. les résultats de l'essai de chargement à pleine échelle réalisées sur les micropieux sont présentés et analysés en termes de courbes de charge. Les résultats de l'essai monotone que les valeurs géotechniques force de liaison proposée par le manuel d'implantation FHWA (2000) pour les dépôts limono-argileux peut être sous-estimés lors de l'examen micropieux à âme creuse de Type B micropieux injection.

1 INTRODUCTION

A micropile is a small diameter (typically less than 300 mm) drilled and grouted pile that is typically reinforced (FHWA 2000). It is constructed by drilling either an open or cased hole, placing a steel reinforcing element into the borehole and grouting the borehole by gravity, under pressure methods or by a combination of both (post grouting). Micropiles have several advantages: they can be installed in limited head room areas using small drilling equipment at any angle causing minimal disturbance to adjacent structures, they allow a fast installation process, and provide a high grout to soil bond strength.

A new generation of micropiles was developed in the 1980s and is termed “The Titan Injection Bore (IBO) micropile. The IBO utilizes a continuously all threaded hollow steel bar as the drilling and grouting conduit, which allows the pile to be drilled and grouted simultaneously without the need of a casing during drilling. A sacrificial bit with openings that allow for pressure grouting of the surrounding soil is threaded onto the end of the hollow bar and is left in place following drilling. A drilling fluid (air, water, or grout) is introduced through the hollow bar and allows the spoils to flush from up the borehole. This also improves the density and support capability of the surrounding soil.

Despite the growing demand on hollow core bar micropiles, little work has been devoted to evaluating the nominal bond strength, α_{bond}, especially in clayey soils, between the micropile grout and the surrounding soil. The hollow bar micropile type is typically classified as Type B grouting according to the FHWA (2000 guidelines. Gomez et al. (2007) and Mitchell et al. (2007) analyzed the results many field load tests, and conclude that the bond strength values suggested by the FHWA (2000) for Type B seem to be conservative when applied to this type for most soil deposits.

The deviation of the bond strength of the hollow core bar micropiles from that of Type B micropiles may be because the classification didn’t account for the different factors affecting the hollow bar micropiles installation. These factors include: the type of fluid used during installation, the speed and pressure used during installation and during grouting (dynamic grouting), and the effect of these factors on the surrounding ground. Telford et al. (2009) stated that the results of verification testing on hollow core micropile confirm the capability of the micropile to support high compression and tensile loads with small pile head movement.

A field study on the performance of hollow core micropiles in cohesive soils is presented herein. The aim of this study is to evaluate the geotechnical performance of micropiles under monotonic axial loading, with a special emphasis on evaluating the value of bond strength between the grout and surrounding soil. The field study is a part of a comprehensive investigation of the

performance of hollow core micropiles under different types of load and in different configuration; single and pairs of micropiles.

2 TEST SITE CONDITIONS

The piles were installed and tested at the University of Western Ontario Environmental Site. Two boreholes were conducted as part of the current study, within the area where the piles were installed and load tested, and are located 16.6 meters apart. The soil stratigraphy interpreted from the two boreholes, SPT values and the locations of the tested micropiles are given in Figure 1.

The soil deposit consists of clayey silt to silty clay till, from the ground surface to a depth of 5.7m. Significant seams of gravel and traces of small cobbles have been observed during soil exploration. A layer of compact to dense sand with seams of silt appeared up until the end of the available boreholes depths (8.8m). The groundwater table was found at a depth varying from 3.7 to 4.0 m below the ground surface at the time of boreholes.

As the piles were loaded in a rapid fashion, and due to the cohesive nature of the soil, a total stress analysis is used to represent the shear strength parameters in such soils

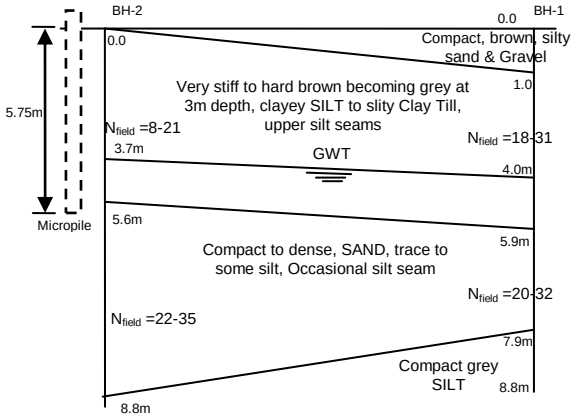

Figure 1. Soil stratigraphy

Several attempts were made to extract undisturbed samples from the boreholes using a thick wall Shelby tube at depths up to 5.7m. All attempts failed in borehole 1 due to the fissured over-consolidated nature of the silty clay soil. The seams of gravel contributed to this failure due to the low recovery ratio. In borehole 2, samples were successfully extracted from depth between 3 to 5.0m. Below depth of 5.7m, the deposit is almost cohesionless and the SPT values were deemed sufficient to evaluate its shear strength. However, because the embedded lengths of micropiles are 5.75 m, the contribution of the silty sand soil to the shaft resistance of the pile is insignificant.

The samples extracted using the Shelby tubes were tested in a triaxial cell under unconsolidated undrained condition (UU). For the shear strength parameter, S_u, to be representative, it was important to use a loading rate during the UU triaxial tests that is compatible with the rate at which the tested pile is displaced during the load test. Therefore, all triaxial tests were conducted at strain rate equal to 0.051mm/min. Table 1 summarizes the results of the three triaxial tests conducted.

Table 1. Summary of unconsolidated undrained triaxial tests results

Depth m	Undrained Shear Strength S_u, kPa	Undrained Secant Modulus, $E_{u50\%}$, MPa	Failure Strain
3.0	86	10.1	6.0 %
3.80	183	23.3	6.0%
4.20	174	22.6	5.66%

3 MICROPILE MATERIALS AND INSTALLATION

The tested micropiles consist of 6m Geo-drilled injection bar, shown in Figure 2.The injection Bar is made of high strength-impact resistant heavy wall steel tubing conforming to ASTM A519. The hollow core bars were supplied in 3m sections and coupled together with 251 mm long coupler, to reach the desired length. The injection bar used had an outer diameter of 76mm, and an inner diameter of 48mm.

The all-thread bar used had a specified yield stress of approximately 580 MPa at a cross-sectional area of 2503 mm^2. A 176mm diameter tungsten carbide blades drill bit was used to advance the hollow core bar down the hole. This bit was chosen in order overcome the gravels and cobbles observed during the soil investigation program. The micropiles were constructed using an excavator mounted TE 550 Hydraulic Drifter.

During drilling, the air-flush technique was used to undercut the soils and flush the drill cutting to the ground surface. Air flushing, rather than the continuous flushing grout technique, was employed in order to examine its ability to advance the hollow core bar down hole with the same efficiency as grout flushing and without any losses in the grout material. This technique can be successful in cohesive deposits.

During air flushing, the hollow core of the all-thread bar is connected to an XAS 375 JD6 portable air compressor through the swivel at the top of the drilling rig. A controlled pressure of between 0.9 and 0.96 MPa was used to advance the hollow core bar downward and flush the debris out from the top of the hole. After reaching the desired depth, the swivel at the top of the drifter was changed and connected to the grout plant

The bar was grouted continuously to fill the annulus between the hollow core bar and the surrounding soil using a universal post-tensioning grout, Master Flow 1341 grout. The grout used has water cement ratio of about 0.32 supplied by the grout plant at a pressure of approximately 1.9 MPa The grout cylinders obtained during the installation process were tested after 7 and 28 day for compression and tensile strength. Table 2 shows the results of the tested grout samples.

Following the previous procedure, four micropiles were installed in the same day in a square arrangement,

Figure 2. B7X1-76 Geo-drilled hollow core injection bars

and were spaced at 776mm center to center as demonstrated in Figure 3. The micropiles were left for curing after installation for more than 5 weeks before testing commenced.

Table 2. Grout strength

	Compression Strength, MPa	Tensile Strength ,MPa
7 days	18.6	4.2
28 days	30.0	6.5

4 INSTRUMENTATION AND TEST SETUP

4.1 Load Test Setup

A reaction frame system was used to execute the pile load tests as shown in Figure 4. The reaction frame involved two steel reaction beams, main and secondary, anchored to four helical screw piles that were used as reaction piers.

The main beam is 4.5 m long and consists of two C380X50 connected back to back with a spacing of 86 mm. The two beams are connected with plates of dimensions 300X400X25.4 mm at an interval of 500 mm. The secondary beam is 4.0 m long and consists of two C380X50 connected back to back with at a spacing of 51mm. They are connected together by two C310X31 face to face; one at the top of the main channels and one at the bottom.

The anchor piles were located at 2.0m from the center of the tested micropile (i.e. at a distance greater than 10 times the tested micropiles diameter). The load was applied using a hydraulic jack with a maximum capacity of 980 kN and 150mm stock, located above the pile head and reacting against the reaction frame. The load was measured using a load cell with a maximum capacity of 890 kN located between the pile head and the loading jack. The load cell was situated on top of a 40 mm thick and 300 mm square steel plate attached to the pile head

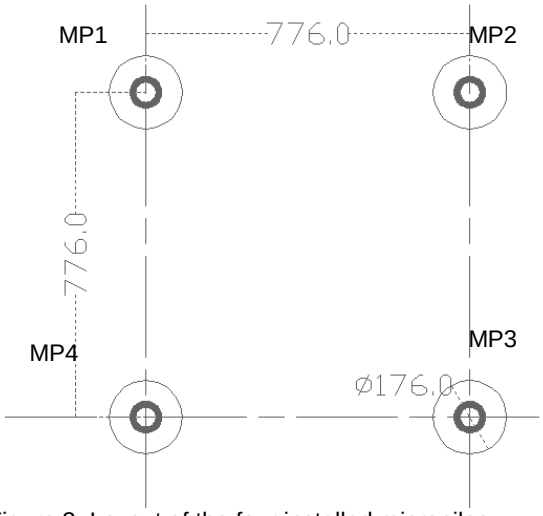

Figure 3. Layout of the four installed micropiles

4.2 Pile Instrumentation

Each micropile was instrumented by five embedded vibrating wire strain gages spaced at 1.5 m from each other. The hollow core steel is consisting of all thread bars from outside and smooth steel surface from inside. At the time of preparation for installation, there was a concern that if the strain gages installed inside the hollow core of the bar a separation between the grout inside and the steel may occur when the loads during the tests reach high values. At this case, the data will be inconsistent.

The concern was due to the apparent weak bond between the grout inside the bar and the smooth surface of the steel. Hence, the strain gages were installed at the outer annulus between the all thread bars bar and the grout. Due to some installations problems, only the top two strain gages survived. The two survived gage were located at the top of the micropile and at depth of 1.5m below the pile butt. A further discussion about the results is given in the following section.

Four linear displacement transducers (LDT) were used to measure the movement of the pile head. The LDTs had 100 mm stroke with an accuracy of 0.01 mm. The LDTs were distributed in a square arrangement over the steel plate attached to the pile head. The LDTs were mounted on two reference steel extensions supported independently from the loading system. The load cell and the LDTs were connected to a data acquisition system to record and store the load and movement at the pile head during the load test.

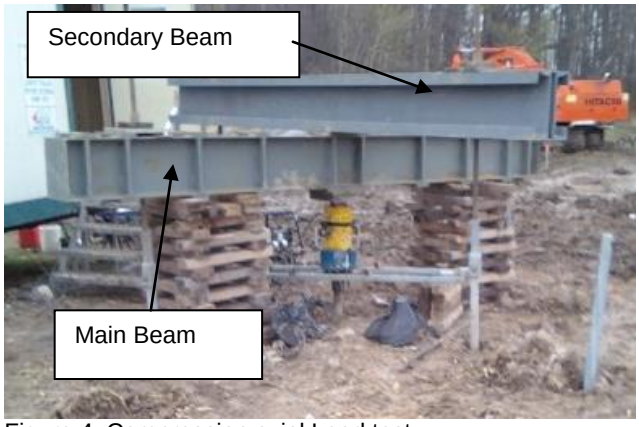

Figure 4. Compression axial Load test

5 MONOTONIC AXIAL TEST AND RESULTS

Two compression load tests were conducted on micropiles MP1 and MP3 in sequence, followed by the tension tests conducted on MP2 and MP4. A finial compression test was conducted on MP2. A quick maintained load test procedure was considered in this study, where the load was applied in increments and each increment was maintained for a period of time.

Generally, the micropiles were tested in compression in accordance with the ASTM D1143 (1994) quick maintained load test procedure. In tension, they were tested in accordance to ASTM D-3689 (2007) quick maintained load test procedure.

Due to the relatively close spacing between the piles (spacing to diameter ratio, S/D =4.4), and because the cohesive nature of the soil deposits, a long testing schedule was followed. The testing schedule incorporated a waiting period of at least 10 days between any two consequent tests to allow the soil surrounding the piles some time to rest and regain strength.

The piles were loaded monotonically, where each load increment was applied and maintained for at least 5 minutes until the maximum load of the test was achieved. When the pre-specified maximum load was reached, a 10 min creep test was conducted in accordance with the guidelines of the Post-tensioning Institute (2004) to examine the geotechnical failure of the piles

One of the main objectives of this study is to highlight the importance of considering the behavior and performance of this type of micropiles geotechnically rather than structurally. The bond at the bar / grout interface is not an issue for all thread bars used nowadays in micropiles. It is always the grout / ground interface that is the limiting factor.

In accordance with the FHWA (2000) Micropile Design Manual, structurally, the installed micropiles can be tested to a load of 1570 kN in compression and a load of 1160 kN in tension using a factor of safety of 1.25. From a geotechnical prospective, FHWA (2000) considers the hollow core micropile as Type B micropile, pressure grouted. Hence, the nominal bond strength of the stiff silty clay deposit present in the test site would be between 70 and 190 kPa.

Given the S_u values obtained from the soil investigation program, the highest bond value should be considered because of the high value of S_u. Therefore, the theoretical ultimate geotechnical capacity of the micropiles with 176 mm diameter was expected to be 600 kN for either compression or tension loading. Therefore, the pile load test was carried to a maximum load at the pile head equal to 600 kN.

Figures 5 and 6 show the load-displacement curves for the three compression and the two tension tests, respectively. Micropile MP2 was loaded monotonically in tension first then in compression. Figure 5 shows that the responses of MP1 and MP3 are almost identical, while MP2 shows a more flexible response especially at the beginning of loading. This may be attributed to the fact that the pile was loaded in tension prior to the compression load test. Hence, its compression behavior was affected by a permanent upward displacement. The result was a relatively larger displacement at the beginning of the compression load test. As the compressive loading continued, the stiffness increased and became similar to that of MP1 and MP3.

Figure 6 reveals that the two tension piles behave differently. Micropile MP2 displayed a stiffer response compared to MP4. Nonetheless, the two piles, as well as the piles tested under compression were loaded to a maximum load between 575 and 600 kN with no signs of approaching failure. This demonstrates that the α_{bond} suggested by the FHWA (2000) for Type B micropile underestimates the hollow core micropiles geotechnical capacity.

It was anticipated that the results from the two survived strain gages at each pile would give more data on the load transfer mechanism at the top of the pile and the change of stiffness modulus of the grout with different loading stages. Unfortunately, the data obtained from the strain gages was found to be inconsistent, as it changes from compression to tension during the monotonic axial compression tests. This may be attributed to a tilt in the axis of the strain gage with the vertical during installation.

It was observed that no slippage took place between the grout inside the hollow core and the enclosing bar, which was the concern of inserting the strain gages inside the bar. Accordingly, It is recommended for further field load tests on this type of micropiles to install the strain gages inside the hollow core bar, after installation and before grouting, with no concern of slippage occurrence unless structural failure of the pile shows up.

To examine the possibility of failure of the tested micropiles, the results are examined using two ultimate load criteria: Davisson offset limit (1972) (considered conservative) and NYSDOT (2007) criterion. The Davisson offset limit failure criteria states that the deflection at failure load is:

$$S_f = e_s + 4.0 + D/120 \quad [1]$$

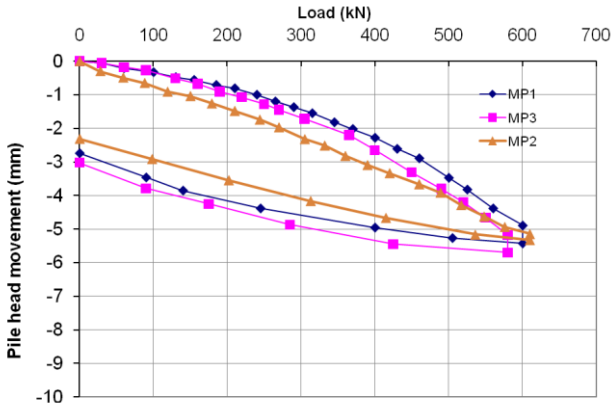

Figure 5. Load–deflection curve for three compression tests

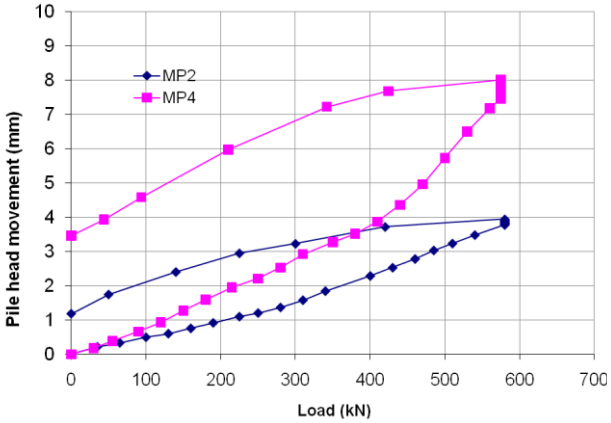

Figure 6. Load –deflection curve for two tension tests

Where: S_f is the deflection at the ultimate load, e_s is the amount of elastic shortening of the pile, and D is the pile diameter (in mm). The amount of elastic shortening of the pile depends on the load transfer mechanism from the pile to the surrounding soil. Generally, e_s, is computed from (FHWA (1992)):

$$e_s = (Q_b + \alpha_s Q_s) \frac{L}{A_p E_p} \quad [2]$$

Where: L is the pile length, A_p is the gross cross section area of the pile, E_p is modulus of elasticity of the pile, Q_b is the load transmitted at the pile tip, Q_s is the load transmitted at the pile shaft, and α_s is a coefficient depending on the nature of unit friction resistance distribution along the pile shaft (e.g. uniform or linear distribution). For no load transfer via shaft resistance (End bearing piles), $\alpha_s = 0.0$.

In the case of micropiles, most of the load is transferred to the soil through shaft resistance, relying on the strong grout/ ground bond developed during installation and grouting. A micropile is believed to reach geotechnical failure when reaching an end bearing condition. Accordingly, it is reasonable to assume the value of Q_b to be zero in this case. Due to the over-consolidation behavior of the cohesive soil deposit at the site, a uniform distribution of the shaft friction is considered, and α_s was taken equal to 0.5.

The elastic shortening of the pile, e_s, is a function of its axial stiffness, E_pA_p. The axial stiffness of a micropile subjected to tensile loads can be evaluated in a simplified manner by treating it as an anchor, considering its single reinforcing core without accounting for the contribution of its grout. For tension test, the axial stiffness is

$$\Sigma (EA)_{tension} = E_{bar} \text{ X } A_{bar} \quad [3]$$

Where: $(EA)_{tension}$ is the axial tension stiffness of the micropile, E_{bar} is modulus of elasticity of the steel = $2x10^5$ MPa, A_{bar} is cross section area of the hollow core bar. The composite stiffness of the micropile in compression is more complicated, due to the many factors involved in the installation process, and the possible contribution of the surrounding soil, but can be simplified as:

$$\Sigma (EA)_{compression} = (E_{grout} \text{ X } A_{grout}) + (E_{bar} \text{ X } A_{bar}) \quad [4]$$

Where: $(EA)_{compression}$ is the axial compression stiffness of the micropile, A_{grout} is the cross section area of the grout and E_{grout} is modulus of elasticity of the grout, which assigned at $2.1x10^4$ MPa

The NYSDOT (2007) failure criteria states that the slope of the load-gross settlement curve at twice the design load shall be 0.15 mm/ kN (i.e. the ultimate load is the load at which the slope of the load-gross settlement curve exceeds 0.15mm/ kN).

Figures 7 and 8 present the load-settlement curves of the tested piles, along with the Davisson's and NYSDOT failure criteria. Figures 7 and 8 demonstrate clearly that the maximum loads of 600 kN for compression piles and 580 kN load for tension piles are well below the specified failure criteria and that no sign of failure was observed. This is further confirmed by the small values of creep recorded at the pile head presented at Table 3.

Considering this observation and analysis of the results and by extrapolation the failure load using Davisson criteria, as illustrated in Figure 7, the average nominal bond strength along the micropile length (at diameter equal to 176mm) is 240 kPa. This value exceed the nominal theoretical bond strength suggested by the FHWA (2000) for Type B micropiles installed in stiff silty clay or clayey silt deposit by a factor of about 25%.

An inspection of the pile diameter enlargement should also be considered due to the dynamic installation process. Using air as a flushing fluid, (a pressure less than 1 MPa during installation), and 2 MPa pressure during grouting in a stiff silty clay deposit may lead to an increase of 15 to 20 %in the pile diameter (William Form –Ground Anchor system 2010).

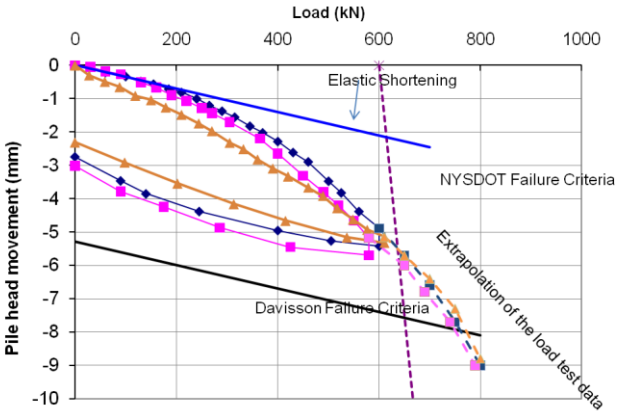

Figure 7. Load –deflection curve for three compression tests with two failure criteria

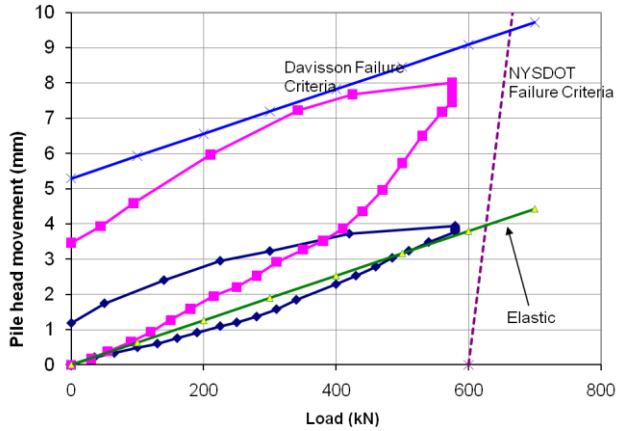

Figure 8. Load –deflection curve for two tension tests with two failure criteria

This increase in the pile diameter must be treated with caution, as it is not uniform along the pile shaft. The increase in pile diameter reaches its maximum value at the pile base, where the grout is pressured through the bit holes at high pressure during grouting, and decreasing until it reaches the bit diameter near the pile head. Taking this factor into consideration, the average nominal bond strength around the micropile will be in the range of 200 to 240 kPa along the pile length depending on the enlargement of the pile diameter.

These results suggest that the hollow core micropiles should be treated, geotechnically, as a new type of grouted micropiles, Type E. This new designation should account for installation conditions such as flushing fluid, pressure used during installation and grouting, and speed of advancing the hollow bar into the ground, as well as the ground type

5.1 Debonding and Apparent Elastic Length

Bruce et al. (1993) proposed the concept of “elastic ratio”, for evaluating micropiles performance. They showed that the measurement of the elastic deflections can be used to evaluate the length of the pile that is being stressed, i.e.

Table 3. Micropiles creep at maximum applied load

	Test	Applied Load P, kN	Creep from 1 to 10 min mm
MP1	Compression	600	0.54
MP2	Tension	580	0.17
MP3	Compression	580	0.53
MP4	Tension	575	0.54
MP2	Compression	610	0.18

engaged in transferring the load through the grout-ground bonding, in order to evaluate the magnitude and distribution of the load transferred to the ground. The elastic ratio, ER, is defined as the ratio between the elastic deformation of the pile (elastic rebound) and the applied load, that is

$$ER = \frac{\delta_e}{\Delta P} \quad [5]$$

Where: ER is the elastic ratio, δ_e is the elastic rebound measured or estimated during unloading cycle, and ΔP is the magnitude of the unloading calculated as the maximum applied load minus the final load after unloading,

Another important parameter that is used to assess the performance of the tested micropiles is the apparent elastic length, L_e, given by:

$$L_e = \frac{\delta_e * \Sigma EA}{\Delta P} \quad [6]$$

Where: L_e is the elastic length of the pile and ΣEA is the combined elastic axial stiffness of the micropile section in compression or the elastic axial stiffness of the steel bar in tension

It should be noted that L_e and ER are intrinsically related; one of them can be used to evaluate the other. The value of δ_e for a pile is estimated for a pile as the total movement minus the residual movement after unloading cycle. Practically, upon unloading, the pile will still have some level of elastic deformation caused by locked-in bond stresses as examined by Gómez et al. (2003). This causes the elastic rebound to be underestimated as well as the load transfer portion of the bond zone, i.e. the apparent elastic length. This behavior is shown clearly during the analysis of the cyclic load test phase presented later on.

For a fully bonded micropile, i.e. no casing zone, the value of L_e can be related to the portion of the micropile subjected to substantial axial load. Hence, it can be used to estimate the ultimate average bond strength of the pile shaft where debonding is most probably to occur.

Table 4. Summary of the monotonic testes phase results

	Test	P_{max} kN	Total Displacement δ_t , mm	Residual Displacement δ_r , mm	Elastic Displacement δ_e , mm	Elastic length L_e, m
MP1	Compression	600	5.43	2.70	2.73	3.88
MP2	Tension	580	3.95	1.18	2.77	2.15
MP3	Compression	580	5.70	3.02	2.68	4.00
MP4	Tension	575	8.00	3.46	4.54	3.70
MP2	Compression	610	5.32	2.31	3.01	4.25

Also, It can be used to assess whether an end bearing condition is developed or not. Bruce et al. (1993) explained the development of the end bearing condition as a probability of micropiles failure, which they attributed to the small diameter of the micropiles. Table 4 illustrates the results obtained from the monotonic test phase on the micropiles by computing the total, residual and elastic movement as well as the corresponding elastic length calculated using Equation 6. It is noted from Table 4 that the developed elastic length is less than the total length for all micropiles. This emphasizes that no-geotechnical failure has occurred for any of the tested micropiles and that the ultimate load is much higher than the maximum load applied during the monotonic load test.

Due to the over-consolidated nature of the stiff silty clay layer, a post-peak behavior may take place along grout/ground interface at the apparent elastic length rather than full debonding of this portion of the micropile, with the rest of the micropile length still contributing to the grout/ground bond strength. This phenomenon could be examined through cyclic load testing. The results of the cyclic load tests will help in assessing whether a full debonding or softening (post-peak behavior) of the micropiles would take place in this type of soils. This may be an important issue for design of micropiles subject to machinery loading, and/or micropiles installed in seismic areas.

6 CONCLUSIONS

Five full scale monotonic load tests were conducted on four instrumented micropiles to investigate the geotechnical behavior of hollow-core bar micropiles. Hollow bars of type BX76 geo-drilled anchors, 76mm OD and 48mm ID were used employing a 176mm carbide bit threaded onto the bar to advance it down the hole. Air flushing technique was used to flush the soil cuttings out of the hole. Three compression and two tension monotonic axial tests were conducted following the quick maintained load test procedure. Based on the results of the study, the following conclusions may be drawn:

1. Categorizing the hollow core micropiles as Type B underestimates the interface bond strength. Hollow core micropiles should be treated as a special grouted micropile. This category should take into consideration factors such as the pressure, speed, and method of installation/flushing, and grouting pressure.
2. The analysis of the loading test results showed that the elastic ratio, ER, and/or the apparent elastic length, L_e, approach can explain the performance of the micropiles monotonically.

ACKNOWLEDGEMENTS

The authors would like to acknowledge the kind support provided by Williams Form Hardware for funding and supplying the steel bars and drilling bits for the project, EBS Engineering and Construction Limited, for installing the micropiles and help setting the reaction frame, and BASF for providing the grout at no cost. Special thanks for Mr. Martin Hodgson from Williams for his technical support throughout the research project

REFERENCES

ASTM Standers D1143-81 1994. Standard Test Method for Deep Foundations Under Static Axial Compressive Load, *Annual Book of ASTM Standards*, ASTM International, West Conshohocken, PA.

ASTM Standers D3689-07 2007. Standard Test Methods for Deep Foundations Under Static Axial Tensile Load, *Annual Book of ASTM Standards*, ASTM International, West Conshohocken, PA.

ASTM Standers A519-06 2006. Stander Specification of Seamless Carbon and Alloy Steel Mechanical Tubing, *Annual Book of ASTM Standards*, ASTM International, West Conshohocken, PA.

Bruce, D.A., Bjorhovde, R., Kenny, J.R. 1993. Fundamental Tests on the Performance of High Capacity Pin Piles, *18th Annual DFI Conference*, Pittsburgh, PA,USA, 1: 1-33.

Davisson, M.T. 1972. High capacity piles, *Soil Mechanics Lecture Series on Innovations in Foundation Construction*, ASCE, Illinois Section, Chicago, USA, 1: 81–112.

Federal Highway Administration 1992. Static Testing of Deep Foundations, *FHWA Publication No. FHWA-SA-91–042*, US Department of Transportation, McLean, VA, USA.

Federal Highway Administration 2000. Micropile Design and Construction Guidelines – Implementation Manual, *FHWA Publication No. FHWA-SA-97–070*, US Department of Transportation, McLean, VA, USA.

Gómez, J.E., Cadden, A.W., Bruce, D.A. 2003. Micropiles in Rock; Development and Evolution of Bond Stresses under Repeated Loading, *12th Pan-American Conference on Soil Mechanics and Geotechnical Engineering*, Essen GMBH, Cambridge, MA, USA.

Gómez, J.E., Rodriguez, C.J., Robinson, H.D., Mikitka, J., and Keough. L. 2007. Hollow Core Bar Micropiles – Installation, Testing, and Interpolation of Design Parameter of 260 Micropiles, *8th International Workshop on Micropile,* Toronto, Canada, CD-ROM.

Mitchell, C.L.B, Mathieson, W.L., and Hopkins, T.W. 2007. Micropile Load Transfer Rates and Bond Stresses in the Puget Sound Region of Washington State U.S.A, *8th International Workshop on Micropile,* Toronto, Canada, CD-ROM.

New York State Department of Transportation 2007. Static Pile Load Test Manual, *Geotechnical Control Procedure GCP-18 Revision 03, Geotechnical Engineering Bureau*, NY, USA.

Post-Tensioning Institute 2004. Recommendations for Pre-stressed Rock and Soil Anchors" Phoenix, AZ. USA.

Telford, W.W., Kokan, M.J., and Aschenbroich, H.K. 2009. Pile Load Tests of Titan injection Bored Micropiles at an Industrial Plant in North Vancouver, *9th International Workshop on Micropile*, London, England, CD-ROM.

Williams Form Engineering Crop 2010. Ground Anchored System, *Publication No. 109*, 8165 Graphic Dr., Belmont, MI 49306, USA.